A New Spectroscopic Approach to Examining the Role of Disulfide Bonds in the Structure and Unfolding of Soybean Trypsin Inhibitor†

Jaclyn Tetenbaum and Lisa M. Miller*

National Synchrotron Light Source, Brookhaven National Laboratory, Upton, New York 11973

Received April 19, 2001; Revised Manuscript Received July 12, 2001

ABSTRACT: Although it is well-known that disulfide bonds stabilize the secondary structure of many proteins, it is difficult to directly probe both disulfide bond formation/breakage and the resulting secondary structural changes during the course of the protein folding/unfolding process. In this work, we have used a new, real-time spectroscopic approach to examine how the reduction of two disulfide bonds affects the secondary structure of soybean trypsin inhibitor (STI). The disulfide bonds are reduced with tris(2-carboxyethyl)-phosphine (TCEP) at 40 °C, and the reduction process is probed in real-time using sulfur X-ray absorption spectroscopy. Circular dichroism (CD) and Fourier transform infrared (FTIR) spectroscopies are used concurrently to determine the structural changes caused by reduction of the disulfide bonds. Results demonstrate a noncooperative reduction of the two disulfide bonds within 5 min, likely because they are located on the surface of the protein. The unfolding of STI lags behind; dramatic changes are not observed until 60−90 min after the reduction was initiated. The CD and FTIR spectra indicate a *decrease* in the amount of extended (hydrated) coil, suggesting that the STI structure slowly collapses after the disulfide bonds are reduced. Thus, although the disulfide bonds are not located near the active site of STI, they play a crucial role in stabilizing the protein structure, which is necessary to sustain enzymatic activity.

One of the most common and important structure-stabilizing motifs in proteins is the disulfide bond. At least 5% of the proteins with known structures contain disulfide bonds between cysteine residues. The strength of the covalent disulfide bond is especially important for proteins formed in the endoplasmic reticulum that will be secreted and exposed to extreme and/or changing conditions such as pH and temperature (*1*). Yet although extremely important, the process of disulfide bond formation and its role in protein folding and stability are not completely understood.

Disulfide bonds are known to stabilize certain serine proteinase inhibitors from Leguminosae seeds. The Kunitz-type proteinase inhibitors contain two disulfide bonds. In soybeans, the Kunitz-type trypsin inhibitor (STI)[1] is thought to be part of a defense mechanism that inhibits insect proteases. It may also be involved in controlling endogenous proteases while the seed is dormant (*2*). Another Kunitz-type proteinase inhibitor, *Erythrina* trypsin inhibitor (ETI), has recently attracted biotechnological interest based on its affinity for tissue-type plasminogen activator (tPA) (*3*). tPA is currently being used as a clot-dissolving agent for stroke and heart attack patients. There is a high degree of homology between Kunitz-type proteinase inhibitors, but substrate specificity and redox behavior vary significantly. For example, unlike ETI, STI is not able to inhibit tPA (*4*, *5*). Thus, it is important to understand the significance of the disulfide bonds for the stability and inhibitory specificity of the protein.

The most common way to examine disulfide bonds in the reductive unfolding (or oxidative folding) of proteins is by chemical derivatization, where the unfolding (or folding) process is halted at various time points and the free sulfhydryl groups are carboxymethylated and analyzed spectroscopically (*6*). However, this method has the disadvantages that chemical derivatization halts the reaction and may also alter the secondary structure of the protein, preventing additional spectroscopic analysis. In this work, we have taken a new and different approach to simultaneously examining (*1*) the redox state of the disulfide bonds and (*2*) the secondary structure of the protein *in real time* during the reductive unfolding of STI. This was done spectroscopically without chemical derivatization by using sulfur X-ray absorption spectroscopy to measure the extent of disulfide reduction, while circular dichroism (CD) spectroscopy and Fourier transform infrared (FTIR) spectroscopy were used simultaneously to probe the changes in secondary structure.

MATERIALS AND METHODS

Sample Preparation. A 0.75 mM solution of soybean trypsin inhibitor (type 1-S, Sigma Chemical Co.) was prepared by adding 22 mg of STI to 3 mL of a 100 mM KP_i/D_2O buffer, pH 6.9 (Aldrich Chemical Co.), and allowing the solution to equilibrate for 24 h. For the model spectra of the sulfur-containing amino acids, 50 mM solutions of each sample were prepared in 100 mM KP_i/H_2O buffer. All

† This work and the NSLS are supported by the U.S. Department of Energy under Contract DE-AC02-98CH10886. J.T. was supported by the U.S. Department of Energy Research Undergraduate Laboratory Fellowship (ERULF) Program.

* Corresponding author. Phone: (631) 344-2091. Fax: (631) 344-3238. E-mail: lmiller@bnl.gov.

[1] Abbreviations: STI, soybean trypsin inhibitor; TCEP, tris(2-carboxyethyl)phosphine; ETI, *Erythrina* trypsin inhibitor; tPA, tissue-type plasminogen activator; PPT, porcine pancreatic trypsin; XAS, X-ray absorption spectroscopy; FTIR, Fourier transform infrared spectroscopy; CD, circular dichroism.

10.1021/bi010796u CCC: $20.00
Published on Web 09/08/2001

solutions were prepared at pH 7 except the cysteine thiolate sample, which was prepared at pH 12.

Reduction of STI. Tris(2-carboxyethyl)phosphine (5 mg) (TCEP, Sigma Chemical Co.) was added to the STI solution (8.8 mM, final concentration). The resulting solution was stirred and warmed to 40 °C in a water bath on a magnetic stirring hot plate. The reaction with TCEP has been shown to effectively reduce the disulfide bonds in proteins (*7*). TCEP was chosen as the disulfide reducing agent because it does not contain sulfur and thus would not interfere with the XAS measurements.

Spectroscopic Analyses. *(A) Sulfur X-ray Absorption Spectroscopy*. X-ray absorption spectroscopy (XAS) was used to measure the extent of disulfide reduction. For the model spectra of the sulfur-containing amino acids, 50 μL of the 50 mM solution of each sample was soaked into a 1 cm^2 piece of type A/E glass fiber filter paper (Gelman Sciences). The filter paper was then sealed in Mylar film (3 μm thick, SPEX) to prevent sample evaporation. For the STI experiment, a 50 μL aliquot was removed from the reaction vessel at each time point and prepared as described for the model compounds. X-ray absorption spectra were collected at Beamline X19A at the National Synchrotron Light Source at Brookhaven National Laboratory using a Si(111) double-crystal monochromator and a downstream rhodium-coated focusing/harmonic rejection mirror. The sample was mounted in a helium-purged sample chamber, and X-ray fluorescence was collected using a PIPS detector (Canberra Industries). Data were collected at room temperature across the sulfur edge from 2462 to 2497 eV in 0.2 eV steps with an integration time of 2 s/point. X-ray spectra were taken of STI aliquots before TCEP was added, just after TCEP was added, and every 30 min for 330 min until the reaction was complete, based on the CD and FTIR spectra. For monochromator calibration, a spectrum of Na_2SO_4 was collected before and after the experiment. The X-ray edge position of Na_2SO_4 was calibrated to 2483 eV. No shifts in the monochromator position were observed throughout the experiment.

Each XAS spectrum was baselined and normalized using Grams 32 software (Galactic Industries). The spectra of disulfide-intact STI (no TCEP) and reduced STI (330 min after the addition of TCEP) were used as end points for the disulfide-intact and disulfide-reduced states, respectively. Linear combination least-squares analysis was performed on the first derivatives of each spectrum. Percent reduction was determined using a linear combination of the first ($t = 0$ min) and last ($t = 360$ min) XAS spectra. The time scale of the reaction was determined by plotting the fraction reduced versus time. Time constants were determined by fitting with Prism software (GraphPad Software, Inc.).

(B) Fourier Transform Infrared (FTIR) Spectroscopy. Samples were prepared by placing a 30 μL aliquot of STI solution (or 30 μL of KP_i/D_2O buffer for the background spectrum) between two BaF_2 windows using a 50 μm spacer. FTIR spectra (128 scans, 4 cm^{-1} resolution) were collected using a dry nitrogen-purged, Nicolet 560 FTIR spectrometer equipped with a DTGS-KBr detector and OMNIC ESP 5.1 software. Spectra were collected from aliquots of the STI solution before TCEP was added, just after TCEP was added, and every 30 min for 360 min until no additional changes in the spectra were observed.

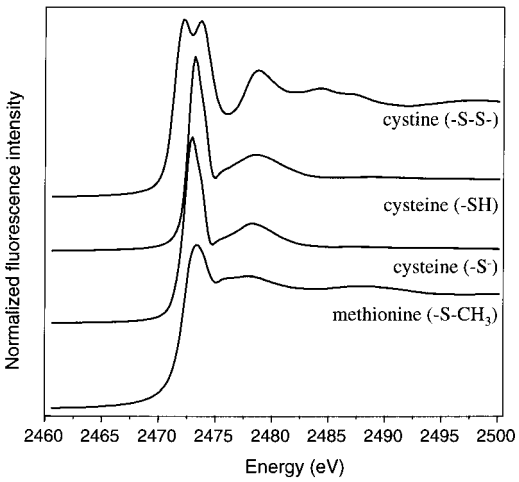

FIGURE 1: Sulfur X-ray absorption spectra of the sulfur-containing amino acids: cystine, cysteine, cysteine thiolate, and methionine. Samples were prepared and data were collected as described in the text.

FTIR data were analyzed using Grams 32 software. The spectra were truncated between 1730 and 1600 cm^{-1} and baseline corrected. Difference spectra were generated by subtracting the spectrum of disulfide-intact STI from the spectra of reduced STI at each time point. The changes in peak frequency and intensity were then assigned to structural changes within the protein (*8*). The time scale of the unfolding process was determined by plotting the change in absorbance versus time for each secondary structure component. Time constants were determined by fitting with Prism software.

(C) Circular Dichroism (CD) Spectroscopy. Samples were prepared by placing a 30 μL aliquot of STI solution between two quartz windows with a 0.02 cm path length. CD spectra (300−180 nm, 0.5 nm steps) were collected using a dry nitrogen-purged Jasco J-715 spectropolarimeter. Spectra were collected from aliquots of the STI solution before TCEP was added, just after TCEP was added, and every 30 min for 330 min until no additional changes in the spectra were observed.

Since CD spectroscopy is particularly sensitive to α-helical content but less reliable at predicting changes in the β-sheet or extended coil structure, popular self-consistent basis set methods (*9*−*11*) were unsuccessful at modeling the changes observed as STI unfolded. Thus, difference spectra were generated by subtracting the spectrum of disulfide-intact STI from the spectra of reduced STI at each time point using Grams 32. The changes in peak frequency and intensity were then compared to the CD spectra of primarily helix, sheet, and coil structures (*12*) to qualitatively interpret structural changes. The time scale of the structural changes was determined by plotting the change in ellipticity versus time at 225 and 200 nm, where the largest spectral changes occurred. Time constants were determined by fitting with Prism software.

RESULTS

Sulfur XAS is sensitive to the oxidation state of sulfur in a protein. Thus, it can be used as a noninvasive spectroscopic technique to probe disulfide redox reactions in real time. To illustrate, Figure 1 contains the XAS spectra of cystine,

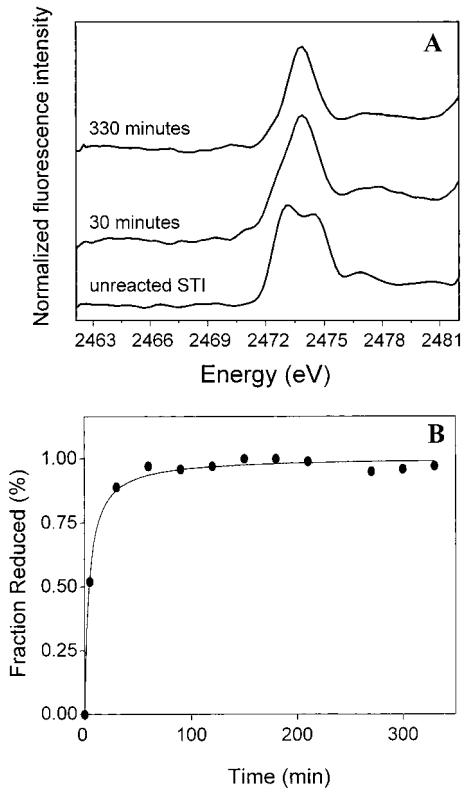

FIGURE 2: (A) Sulfur X-ray absorption spectra of disulfide-intact STI and reduced STI 30 and 330 min after the addition of tris(2-carboxyethyl)phosphine (TCEP) at 40 °C. (B) Linear combinations of fully oxidized and fully reduced STI were used to determine the fraction reduced at each time point. The disulfide reduction in STI was best fit to a single-exponential function, indicating that the reduction of the two disulfide bond was noncooperative and occurred on the same time scale ($k = 0.150$ min^{-1}, $t_{1/2} = 4.6$ min, $R^2 = 0.994$).

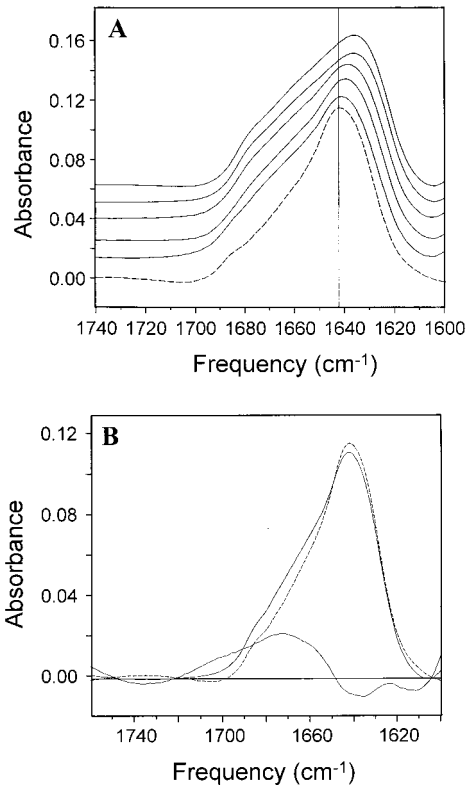

FIGURE 3: (A) FTIR spectra at different time points during the reduction and unfolding of STI. The dashed line represents the spectrum before the addition of TCEP. The solid lines represent spectra collected at various time points after the addition of TCEP: (from bottom to top) 30, 60, 120, 240, and 330 min. The vertical guide line is located at 1642 cm^{-1}. (B) FTIR spectra of unreacted STI (- - -) and STI + TCEP after 5 min (—). The difference spectrum (reduced − oxidized) (magnified 2×) is also shown.

cysteine, and methionine. Since the reduction of cysteine can lead to either the protonated or deprotonated form of the amino acid depending on the pK_a of the cysteine residue, XAS spectra were collected from cysteine (−SH) and cysteine thiolate (−S$^-$). The X-ray absorption spectrum of a sulfur-containing compound without disulfide bonds has a single 1s → σ* (S−C) transition (*13*, *14*), which is observed in the spectra of methionine, cysteine, and cysteine thiolate. The X-ray edge positions of cysteine and methionine were the same, whereas the X-ray edge position of the cysteine thiolate was shifted to lower energy by 0.2 eV. This result is consistent with the increased electronegativity on the deprotonated sulfur atom. The X-ray absorption spectrum of cystine, which contains a disulfide bond, exhibits two absorption features assigned to 1s → σ* (S−S) and 1s → σ* (S−C) transitions. The X-ray edge positions of these features fall ±1.0 eV from the cysteine X-ray edge position.

Native STI, which has two disulfide bonds intact, has two absorption features in the sulfur XAS spectrum, similar to that of cystine (Figure 2A). To use sulfur XAS to probe the disulfide reduction, typical reducing agents that contain sulfur, such as dithiothreitol, cannot be used because they interfere with the XAS measurements. TCEP has been shown to reduce proteins quickly and completely (*7*) and was thus used as the reducing agent for STI. After the addition of TCEP, the 1s → σ* (S−S) transition loses intensity as the disulfide reduction progresses. The fraction reduced at each time point was determined through linear combination fitting of the first derivatives of the XAS spectra. By plotting the fraction reduced as a function of time, we find that the disulfide reduction is complete within 4−5 min after the addition of TCEP (Figure 2B). The time course of the reaction is best fit to a single exponential, where $t_{1/2} = 4.6 \pm 0.4$ min ($R^2 = 0.994$).

Since sulfur XAS is a noninvasive technique, other spectroscopic methods can be used simultaneously to correlate the disulfide reduction to changes in secondary structure. In this work, we have used FTIR and CD spectroscopies to probe the changes in secondary structure as a function of time. Figures 3 and 4 illustrate changes that occur in the infrared spectrum of STI after the addition of TCEP. It has been demonstrated that the amide I band of proteins (1600−1700 cm^{-1}) is sensitive to secondary structure, where α-helices, β-sheets, β-turns, and extended coil structures absorb at different frequencies (*8*). The amide I band of disulfide-intact STI is representative of a protein with high extended coil and β-sheet content, with absorption features at 1645 and 1625 cm^{-1}, respectively. Within 5 min after the addition of TCEP, the FTIR difference spectra illustrate an increase in a broad feature centered near 1670 cm^{-1} (Figure 3). Although high-frequency components in FTIR spectra have been attributed to both β-sheet and turn components (*8*), only turns have *multiple* high-frequency components (*15*, *16*). Since the absorbance change near 1670 cm^{-1} has a width greater than 25 cm^{-1}, we attribute this

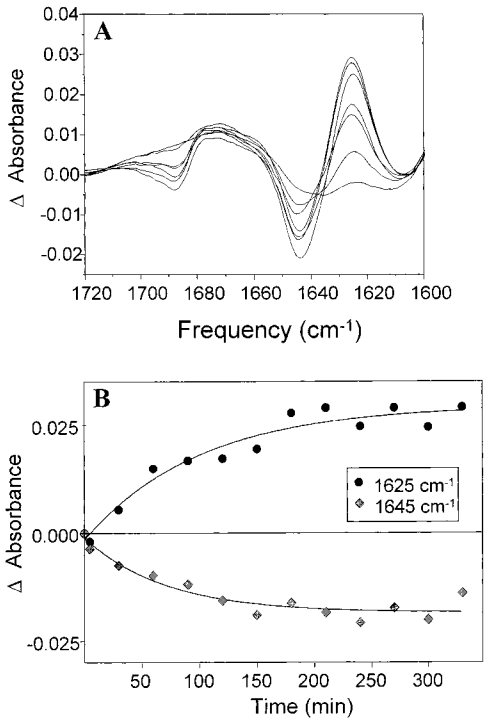

FIGURE 4: (A) FTIR difference spectra (reduced − oxidized) at 5, 30, 60, 120, 240, 270, and 330 min after the addition of TCEP. (B) Absorbance difference and single-exponential fit plotted as a function of time of the disappearance of the feature at 1645 cm^{-1} (◆, $k = 0.014$ min^{-1}, $t_{1/2} = 49.2$ min, $R^2 = 0.905$) and the appearance of the feature at 1625 cm^{-1} (●, $k = 0.010$ min^{-1}, $t_{1/2} = 69.3$ min, $R^2 = 0.950$).

feature to a number of turn components that increase immediately upon disulfide reduction.

After the initial increase in turn content, additional changes in the FTIR spectra lag behind. Specifically, we observe a decrease in the peak intensity at 1645 cm^{-1} ($k = 0.014 \pm 0.004$ min^{-1}, $t_{1/2} = 49.2$ min, $R^2 = 0.905$) and an increase in the peak intensity at 1625 cm^{-1} ($k = 0.010 \pm 0.002$ min^{-1}, $t_{1/2} = 69.3$ min, $R^2 = 0.950$) on similar time scales. Both of these changes can be seen in Figure 4. Absorption features near 1645 cm^{-1} have been assigned to extended (hydrated) coil structures (*17*), whereas β-sheet structures absorb near 1625 cm^{-1} (*18*). Thus, the results demonstrate that disulfide reduction of STI results in a rapid increase in turn content, followed slowly by a loss of extended coil and an increase in sheetlike structure.

In Figure 5A, the changes observed in the CD spectra after the addition of TCEP can be seen. The CD spectra support the structural changes that are observed in the FTIR data. Unlike FTIR spectra, time scales and spectral changes in CD spectra cannot easily be assigned to particular secondary structure elements. However, analysis of model CD spectra (*12*) can provide help with interpreting the spectral changes in STI. Positive and negative features near 200 nm are representative of β-sheet and extended coil conformations, respectively. Thus as STI unfolds, a decrease in a negative feature near 200 nm is consistent with the loss of extended coil and an increase in a sheetlike structure ($k = 0.0073 \pm 0.0014$ min^{-1}, $t_{1/2} = 94.5$ min, $R^2 = 0.965$). Also, for proteins with little α-helical content, negative features near 220 nm are primarily due to the presence of β-sheet structure in the protein. So the observed increase in the negative feature near

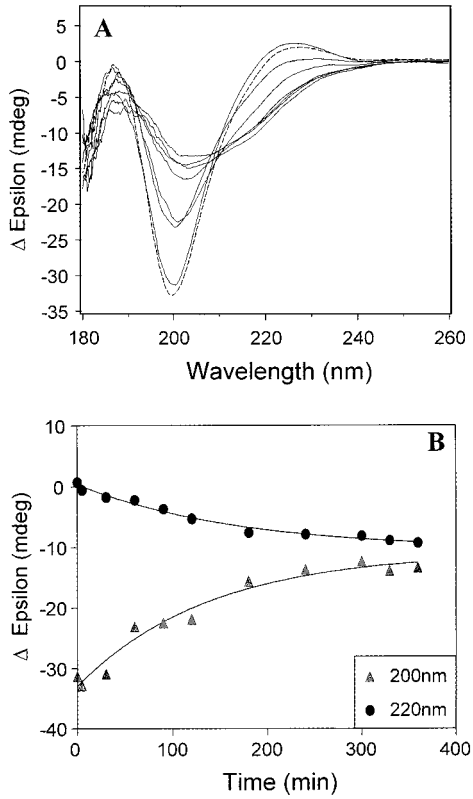

FIGURE 5: (A) CD spectra at different time points during the reduction and unfolding of STI. The dashed line represents the spectrum before the addition of TCEP. The solid lines represent spectra collected at various time points after the addition of TCEP: (from bottom to top) 30, 60, 120, 240, 300, and 330 min. (B) Change in ellipticity at 200 nm (▲, $k = 0.0073$ min^{-1}, $t_{1/2} = 94.5$ min, $R^2 = 0.965$) and 220 nm (●, $k = 0.0059$ min^{-1}, $t_{1/2} = 117$ min, $R^2 = 0.982$) as a function of time.

220 nm also supports an increase in a sheetlike conformation as STI is reductively unfolded ($k = 0.0059 \pm 0.0012$ min^{-1}, $t_{1/2} = 117$ min, $R^2 = 0.982$). Thus, the changes observed in both the FTIR and CD spectra are consistent with a loss of hydrated, extended coil structure and an increase in sheetlike hydrophobic interactions as STI is reductively unfolded.

DISCUSSION

STI is a 20 kDa protein with 181 amino acid residues that was first isolated by Kunitz in 1947 (*19*). The first crystal structure of STI was determined by Sweet and co-workers in 1974 (*20*) and has been refined more recently (*2*, *5*). The secondary structure of STI is approximately 2% α-helix, 38% β-sheet, 23% β-turn, and 37% unordered. STI inhibits porcine pancreatic trypsin (PPT) by forming a stable complex which dissociates very slowly into free trypsin and a modified (cleaved) STI (*21*). The inhibition mechanism has attracted interest recently based on the ability of ETI, another Kunitz-type proteinase inhibitor, to inhibit tPA. Although STI has a high degree of homology to ETI (*22*), it does not inhibit tPA.

STI contains two disulfide bonds (Cys39−Cys86 and Cys136−Cys145) that are located near the surface of the protein, making them highly solvent-accessible. The sulfur XAS results are consistent with the surface location of the disulfide bonds and demonstrate that the disulfide bonds are reduced quickly at 40 °C. Both disulfide bonds are reduced

on the same time scale ($t_{1/2} = 4.6$ min) in a noncooperative fashion (Figure 2). In STI, reduction of the disulfide bonds results in a fully deactivated protein (*4*, *23*). This result is in contrast to ETI, which remains fully active in both the disulfide-intact and reduced states (*4*). Thus, the role that the disulfide bonds play in the stabilization of Kunitz-type proteinase inhibitors is quite varied.

As the disulfide bonds are reduced, the secondary structure of STI begins to change. Within the time scale of the disulfide reduction, the FTIR spectra reveal an increase in the turn content of the protein. However, after this initial change, additional changes in the FTIR spectra lag behind. Specifically, we observe a decrease in the extended (hydrated) coil content and an increase in the β-sheet structure on a time scale of approximately 60 min. These changes are noncooperative and occur on the same time scale within the error of the data. The CD data show similar trends in secondary structure after the disulfide reduction. From these results, we suggest that the disulfide reduction of STI results in a hydrophobic collapse of the protein; the increase in turn content is the first evidence of the collapse, which occurs immediately after the disulfide bonds are reduced. As the collapse proceeds slowly, the extended (hydrated) coil structure is lost and sheetlike hydrophobic interactions increase.

This hydrophobic collapse of STI upon disulfide reduction is in striking contrast to that of ETI. Since the native structures are highly homologous, it is not surprising that the CD spectra of ETI (*4*) and STI are indistinguishable. However, after disulfide reduction, Lehle and co-workers have shown that the CD spectrum of ETI remains unchanged, suggesting that the secondary structure of ETI is not dramatically altered by reduction of the disulfide bonds. In contrast, we find that the CD spectrum of STI changes dramatically upon reduction. These findings are reflected in the activities of the reduced proteins. In the reduced state, ETI remains active (*4*), whereas STI has been shown to be fully inactive (*23*).

Despite the similarities in their overall structures, the surface features of STI and ETI are quite different (*5*). Although both disulfide bonds in STI and ETI are located on the surface of the protein, the structure surrounding each equivalent disulfide bond differs dramatically. For example, the distance between equivalent C^{α} atoms surrounding the Cys39−Cys86 disulfide bond is greater than 6 Å, where the average deviation between all equivalent C^{α} atom pairs is only 2.39 Å. Moreover, the amino acids surrounding this disulfide bond, notably Cys86, are all hydrophobic residues in STI but largely mixed in ETI. Thus, disruption of this disulfide bond could have considerably different consequences between the two proteins. Further examination of the total amino acid content of both proteins indicates that STI has a slightly higher fraction of hydrophobic residues (41%) than ETI (35%), also supporting a higher likelihood of a hydrophobic collapse upon disruption of the Cys39−Cys86 disulfide bond in STI.

In summary, we find that the disulfide reduction of STI is noncooperative and it occurs quickly (<5 min). This likely occurs because both disulfide bonds are located on the surface of the protein, making them highly solvent-accessible. Reduction of the disulfide bonds also results in dramatic changes in the secondary structure of STI, but these changes occur over a longer time scale (5−150 min). The observed structural changes are contrary to those we expected; we hypothesized that disulfide reduction would cause the protein to unfold, resulting in a loss of β-sheet structure and an increase in extended coil content. However, the FTIR and CD data reveal a *decrease* in the amount of extended (hydrated) coil, suggesting that the STI structure is collapsing after the disulfide bonds are reduced. Analysis of the hydrophobic content of the protein reveals that STI contains >40% hydrophobic residues, many of which surround the disulfide bond cysteines. Therefore, we believe that the disulfide bonds are present to prevent a hydrophobic collapse of the protein. This is supported by the fact that, although the disulfide bonds are not located near the active site of STI, all activity is lost upon disulfide reduction (*4*, *23*). Thus, in contrast to ETI which remains active in the disulfide-intact and reduced states, the disulfide bonds in STI play a crucial role in protein structure stabilization necessary to maintain enzymatic activity.

ACKNOWLEDGMENT

The authors acknowledge the technical support of Michael Sullivan, Tony Lenhard, Rick Greene, and Matt Hershcovitch.

REFERENCES

1. Tu, B. P., Ho-Schleyer, S. C., Travers, K. J., and Weissman, J. S. (2000) *Science 290*, 1571−1574.
2. De Meester, P., Brick, P., Lloyd, L. F., Blow, D. M., and Onesti, S. (1998) *Acta Crystallogr. D54*, 589−597.
3. Collen, D., and Lijnen, H. R. (1995) *Thromb. Haemostasis 74*, 167−171.
4. Lehle, K., Wrba, A., and Jaenicke, R. (1994) *J. Mol. Biol. 239*, 276−284.
5. Song, H. K., and Suh, S. W. (1998) *J. Mol. Biol. 275*, 347−363.
6. Wedemeyer, W. J., Welker, E., Narayan, M., and Scheraga, H. A. (2000) *Biochemistry 39*, 4207−4216.
7. Burns, J. A., Butler, J. C., Moran, J., and Whitesides, G. M. (1991) *J. Org. Chem. 56*, 2650−2655.
8. Byler, D. M., and Susi, H. (1986) *Biopolymers 25*, 469−487.
9. Manavalan, P., and Johnson, W. C. (1987) *Anal. Biochem. 167*, 76−85.
10. Sreerama, N., and Woody, R. W. (1993) *Anal. Biochem. 209*, 32−44.
11. Perczel, A., Park, K., and Fasman, G. D. (1992) *Anal. Biochem. 203*, 83−93.
12. Brahms, S., and Brahms, J. (1980) *J. Mol. Biol. 138*, 149−178.
13. Hitchcock, A. P., Bodeur, S., and Tronc, M. (1989) *Physica B 158*, 257−258.
14. Pickering, I. J., Prince, R. C., Divers, R., and George, G. N. (1998) *FEBS Lett. 441*, 11−14.
15. Krimm, S., and Bandekar, J. (1980) *Biopolymers 19*, 1−29.
16. Bandekar, J., and Krimm, S. (1980) *Biopolymers 19*, 31−36.
17. Purcell, J., and Susi, H. (1984) *J. Biochem. Biophys. Methods 9*, 193−199.
18. Susi, H., Byler, D. M., and Purcell, J. M. (1985) *J. Biochem. Biophys. Methods 11*, 235−240.
19. Kunitz, M. (1947) *J. Gen. Physiol. 30*, 311−320.
20. Sweet, R. M., Wright, H. T., Janin, J., Chothia, C. H., and Blow, D. M. (1974) *Biochemistry 13*, 1599−1608.
21. Blow, D. M., Janin, J., and Sweet, R. M. (1974) *Nature 249*, 54−57.
22. Onesti, S., Brick, P., and Blow, D. M. (1991) *J. Mol. Biol. 217*, 153−176.
23. Steiner, R. F. (1965) *Biochim. Biophys. Acta 100*, 111−121.

BI010796U